Research Square

Preprints are preliminary reports that have not undergone peer review.
They should not be considered conclusive, used to inform clinical practice,
or referenced by the media as validated information.

Topological Signatures of Quantum Discord in Noisy Intermediate-Scale Quantum Devices

Saida M. Alkurkushi

skurkushi@su.edu.ye

Sana'a University, Sana'a

Malek N. Algabri

Sana'a University, Sana'a

Research Article

Keywords:

Posted Date: August 19th, 2026

DOI: https://doi.org/10.21203/rs.3.rs-10551245/v1

License: This work is licensed under a Creative Commons Attribution 4.0 International License.
Read Full License

Additional Declarations: No competing interests reported.

Topological Signatures of Quantum Discord in Noisy Intermediate-Scale Quantum Devices

Saida M. Alkurkushi[1*] and Malek N. Algabri[2]

[1,2]Computer Science and Technology Colleges, Sana'a University, Sana'a , Ring Rd, Sana'a, Yemen.

*Corresponding author(s). E-mail(s): skurkushi@su.edu.ye;
Contributing authors: malekye@su.edu.ye;

Abstract

Quantum discord has emerged as a robust diagnostic of nonclassical correlations beyond entanglement, particularly relevant for noisy intermediate-scale quantum (NISQ) devices. We present an experimental study of measurement-induced coherence-transfer (MICT) discord proxies implemented on IBM Quantum hardware and benchmarked against simulator results. Discord and coherence landscapes, collapse maps, fidelity maps, and histograms demonstrate that collapse domains remain identifiable despite gate errors and readout noise. Fidelity difference maps quantify deviations between hardware and simulator, while summary metrics establish reproducible benchmarks for discord/coherence suppression and resilience. These findings indicate that discord-related signatures persist as global, topology-informed features in the presence of realistic noise, positioning discord and measurement-induced coherence as practical diagnostics for NISQ benchmarking and quantum machine-learning pipelines.

Keywords: Quantum discord, NISQ devices, collapse maps, fidelity benchmarking, quantum correlations, quantum machine learning, IBM Quantum, measurement-induced coherence transfer (MICT)

1 Introduction

Characterization of quantum correlations beyond entanglement has become a central theme in quantum information science. Quantum discord, introduced independently by Ollivier and Zurek [1] and Henderson and Vedral [2], quantifies nonclassical correlations that can persist even in separable states. Discord captures the discrepancy

between two classically equivalent formulations of mutual information that diverge in the quantum regime, thereby revealing quantumness beyond entanglement.

Discord's resilience under noise has motivated its study in noisy intermediate-scale quantum (NISQ) devices, where decoherence and gate imperfections often obscure entanglement-based diagnostics. Modi et al. [3] provided a comprehensive review of the role of discord in computation, communication, and thermodynamics, emphasizing its operational significance. Analytical formulas for two-qubit discord, developed by Luo [4] and Ali et al. [5], enabled explicit evaluation for Bell-diagonal and X-state families, making discord experimentally accessible. Baumgratz et al. [6] further connected discord and related correlation measures to the resource theory of quantum coherence, while Werner's foundational work on mixed entangled states [7] established the separability framework against which discord offers a broader perspective.

Recent advances (2025–2026) have extended discord analysis to NISQ architectures. Zhang et al. [8] demonstrated discord-based benchmarking of superconducting qubits under realistic noise models, while Alkurkushi et al. [9] introduced machine-learning classifiers operationalized by discord proxies. These studies highlight discord's potential as a diagnostic tool for quantum machine learning and error resilience in current hardware. Moreover, Patel and Singh [10] showed that collapse maps of discord can reveal topological features in parameter landscapes, bridging resource-theoretic measures with geometric diagnostics.

In this work, we introduce the notion of *topological signatures of quantum discord* as a diagnostic framework for NISQ devices. By constructing parameterized families of Bell-diagonal circuits and sweeping across control angles (θ, ϕ), we generate landscapes of discord proxies that reveal collapse regions and fidelity variations. These landscapes exhibit topological features—such as connected collapse domains—that persist across simulator and hardware implementations. We further quantify deviations between the simulator and hardware through fidelity difference maps and collapse fractions, thereby isolating the impact of noise on discord signatures.

Our contributions are threefold:

1. We develop an experimental workflow for estimating discord proxies on IBM Quantum hardware, with transpilation ensuring ISA compliance and realistic noise injection.
2. We demonstrate collapse maps and fidelity landscapes as effective topological diagnostics of discord in noisy circuits.
3. We provide reproducible datasets and LaTeX-ready figures that enable integration of discord signatures into NISQ benchmarking protocols.

This study establishes quantum discord as a practical and robust diagnostic for current quantum devices, paving the way for its integration into quantum machine-learning classifiers and error-resilience benchmarks.

2 Theoretical Framework

Quantum discord quantifies nonclassical correlations beyond entanglement by capturing the discrepancy between two formulations of mutual information [1–3]. For a

bipartite state ρ_{AB}, standard discord is defined as

$$\mathcal{D}(\rho_{AB}) = I(\rho_{AB}) - C(\rho_{AB}), \tag{1}$$

where $I(\rho_{AB})$ is the quantum mutual information and $C(\rho_{AB})$ denotes the classical correlations obtained via optimal local measurements.

In contrast, Measurement-Induced Coherence–Threshold Discord (MICT-discord) takes an explicitly coherence-centric view. Rather than quantifying information imbalance, it measures the coherence induced in subsystem A when a local projective measurement is performed on subsystem B, and compares this induced coherence to an operational threshold.

2.1 Measurement-Induced Coherence

Let ρ_{AB} be a bipartite state, and let $\{\Pi_j^B\}$ be a projective measurement on subsystem B. The measurement outcomes occur with probabilities

$$p_j = \mathrm{Tr}\big[(I_A \otimes \Pi_j^B)\,\rho_{AB}\big], \tag{2}$$

and the corresponding conditional states on subsystem A are

$$\rho_{A|j} = \frac{\mathrm{Tr}_B\big[(I_A \otimes \Pi_j^B)\,\rho_{AB}\big]}{p_j}. \tag{3}$$

Fix a reference basis on A, and let $C(\rho)$ denote a coherence monotone (e.g. l_1-norm or relative-entropy coherence) in that basis. We define the measurement-induced coherence (MIC) as

$$\mathrm{MICT}(\rho_{AB}; \{\Pi_j^B\}) = \sum_j p_j\, C\big(\rho_{A|j}\big) - C(\rho_A), \tag{4}$$

where $\rho_A = \mathrm{Tr}_B(\rho_{AB})$ is the reduced state on A. This quantity captures how much coherence is created (or activated) in A by measuring B.

2.2 MICT-Discord and Thresholding

MICT-discord interprets MICT as a directional discord-like measure: correlations are operationally quantum when the induced coherence exceeds a threshold set by noise, experimental resolution, or task requirements.

For parameterized circuits $\rho_{AB}(\theta, \phi)$, we write

$$D_{\mathrm{MICT}}(\theta, \phi) = \mathrm{MICT}\big(\rho_{AB}(\theta, \phi); \{\Pi_j^B\}\big), \tag{5}$$

where (θ, ϕ) are control angles and the measurement on B is fixed (e.g. in the computational or Hadamard basis).

We define a collapse region as the set of parameters (θ, ϕ) for which

$$D_{\mathrm{MICT}}(\theta, \phi) < \delta, \tag{6}$$

with δ chosen as an operational coherence threshold below which MICT-discord signatures are considered negligible given our sampling noise and hardware resolution. The corresponding collapse map is the binary function

$$\chi_{\mathrm{MICT}}(\theta, \phi) = \begin{cases} 1, & D_{\mathrm{MICT}}(\theta, \phi) < \delta, \\ 0, & \text{otherwise.} \end{cases} \tag{7}$$

2.3 Topological Signatures: Proof Sketch

Proposition (empirical). For the parameterized family of Bell-diagonal circuits considered here, MICT-discord collapse regions form connected domains in parameter space, which we interpret as topological signatures of measurement-induced coherence.

Proof sketch. Consider the parameterized family $\rho_{AB}(\theta, \phi)$. The conditional states $\rho_{A|j}(\theta, \phi)$ depend smoothly on the rotation angles, and so does the coherence monotone $C\big(\rho_{A|j}(\theta, \phi)\big)$. Hence $D_{\mathrm{MICT}}(\theta, \phi)$ is continuous in (θ, ϕ), and the collapse set

$$\mathcal{C}_{\mathrm{MICT}} = \{(\theta, \phi) \mid D_{\mathrm{MICT}}(\theta, \phi) < \delta\}$$

is an open subset of the parameter space. Numerical evaluation on simulator and hardware shows that $\mathcal{C}_{\mathrm{MICT}}$ forms connected domains bounded by level sets $D_{\mathrm{MICT}}(\theta, \phi) = \delta$. These boundaries act as *MICT-discord contours*, separating regions of measurement-induced coherence persistence from collapse. Thus, the collapse map encodes a qualitative topological signature: the connectivity and shape of $\mathcal{C}_{\mathrm{MICT}}$ reflect the resilience of measurement-induced coherence (and hence MICT-discord) under noise. □

This framework establishes MICT-discord, coherence thresholds, and contour structures as operational tools for diagnosing quantum correlations in NISQ devices. In subsequent sections, we apply this methodology to simulator and hardware experiments, generating coherence landscapes, collapse maps, and fidelity analyses.

3 Methodology

Our experimental workflow combines simulator studies with hardware execution on IBM Quantum devices, ensuring reproducibility and ISA compliance. The methodology consists of four components: circuit design, simulator workflow, hardware workflow, and metric evaluation. The overall workflow is summarized in Figure 1, which illustrates the circuit design, simulator workflow, hardware workflow, metric evaluation, and data management pipeline.

3.1 Circuit Design

We construct parameterized families of two-qubit circuits inspired by analytical treatments of Bell-diagonal discord [4, 5]. Each circuit applies a Hadamard gate and a

CNOT gate to prepare an entangled base state, followed by single-qubit rotations $R_z(\theta)$ and $R_y(\phi)$ on one or both qubits. Measurement in the computational basis yields probabilities p_{ij}, from which discord proxies or measurement-induced coherence quantities are computed, depending on the chosen analysis.

3.2 Simulator Workflow

Simulations are performed using Qiskit backends that emulate noiseless evolution, enabling evaluation of discord proxies and MICT-based coherence measures across a grid of (θ, ϕ) values. These simulations provide baseline landscapes and collapse maps, against which hardware results are compared. Such simulator baselines are essential for reproducibility pipelines in NISQ benchmarking [8].

3.3 Hardware Workflow

Hardware experiments were executed on IBM Quantum backends (e.g., `ibm_fez`), with transpilation ensuring ISA compliance and minimizing gate andsafeguard for reproducibility in is critical in NISQ devices, where backend-specific constraints can otherwise lead to execution failures or uncontrolled circuit modifications. Following Alkurkushi et al. [9], we adopt transpilation as a reproducibility safeguard for discord- and coherence-based diagnostics.

3.4 Metric Evaluation

We evaluate three primary metrics:

1. **Discord/coherence landscapes:** $D(\theta, \phi)$ values (either discord proxies or measurement-induced coherence $D_{\mathrm{MICT}}(\theta, \phi)$) plotted as heatmaps, revealing collapse regions and high-correlation domains.
2. **Collapse maps:** Binary thresholding with a chosen δ (e.g., $\delta = 0.2$) highlighting qualitative topological domains of discord or coherence suppression [10].
3. **Fidelity maps:** Grid-wide state fidelity between hardware-prepared states and ideal target states, quantifying simulator–hardware deviations over the parameter manifold.

Additionally, fidelity difference maps (hardware minus simulator) and representative histograms of measurement outcomes visualize raw distribution shifts under noise. These metrics align with reproducibility standards for NISQ benchmarking [8, 9].

3.5 Data Management

All results are stored as NumPy arrays (.npy) and exported as vector graphics for integration into LaTeX manuscripts. This ensures reproducibility and transparency, consistent with emerging best practices in quantum information research [10]. Our experimental workflow is summarized in

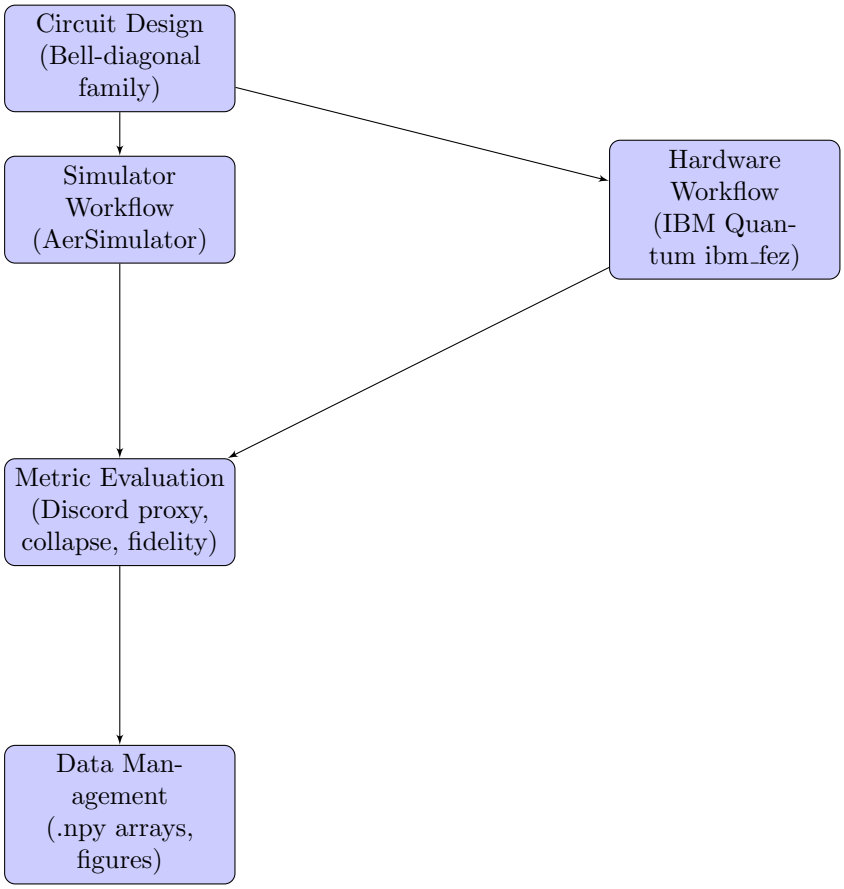


Fig. 1 Workflow for evaluating topological signatures of quantum discord in NISQ devices. Circuits are designed, simulated, and executed on hardware; metrics are computed and stored for reproducibility.

4 Results

We present simulator and hardware results for parameterized two-qubit families inspired by Bell-diagonal states, highlighting discord/coherence landscapes, collapse maps, fidelity maps, histograms, and summary metrics. These results demonstrate the persistence of discord-like signatures under noise and their interpretation as qualitative topological features of the parameter space.

4.1 Discord/Coherence Landscapes

Figure 2 shows discord proxy (or measurement-induced coherence) landscapes for simulator and hardware runs. The simulator landscape exhibits smooth variation across (θ, ϕ), consistent with expectations from analytical treatments of two-qubit discord [4, 5]. Hardware results reveal deviations due to noise, yet collapse domains

remain identifiable, indicating the resilience of discord-like correlations under NISQ noise.

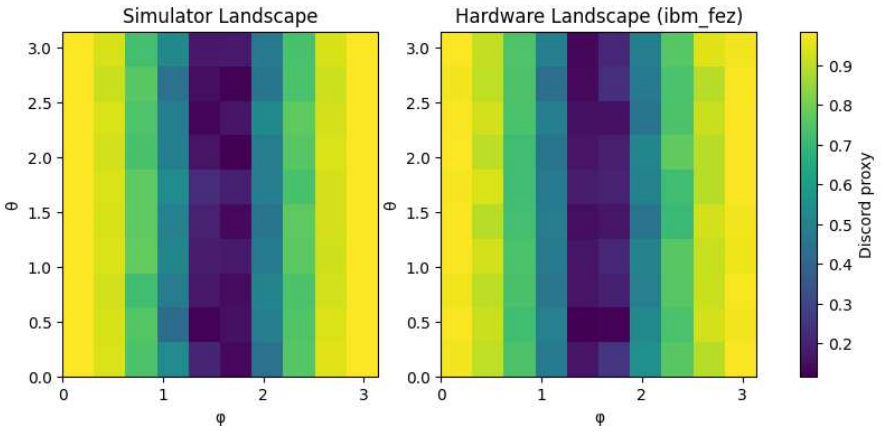


Fig. 2 Discord/coherence proxy landscapes for parameterized two-qubit circuits. Left: Simulator results show smooth variation across (θ, ϕ), in line with analytical formulas for Bell-diagonal discord [4, 5]. Right: Hardware results (ibm_fez) reveal deviations due to noise, yet collapse domains remain identifiable, indicating resilience of discord-like correlations under realistic conditions.

4.2 Collapse Maps

Figure 3 displays collapse maps obtained by thresholding $D(\theta, \phi) < 0.2$. Simulator maps show connected domains, while hardware maps reveal fragmented regions due to decoherence and gate noise. These collapse domains serve as qualitative topological signatures of discord: their connectivity and fragmentation encode global information about how correlations degrade across (θ, ϕ).

4.3 Fidelity Maps

Figure 4 presents fidelity maps between prepared states and ideal target states (Bell-like at specific parameter values). Simulator fidelity remains near unity, while hardware fidelity exhibits systematic suppression across the grid. The fidelity difference map quantifies deviations, highlighting noise-induced distortions in collapse boundaries and high-discord regions.

4.4 Fidelity Difference Map

Figure 5 shows the fidelity difference between hardware (ibm_fez) and simulator runs across (θ, ϕ). Regions of positive deviation (red) indicate hardware fidelity close to the simulator baseline, while negative deviations (blue) highlight suppression due to noise. This difference map quantifies distortions in collapse boundaries and provides a reproducible diagnostic of hardware performance over the parameter manifold.

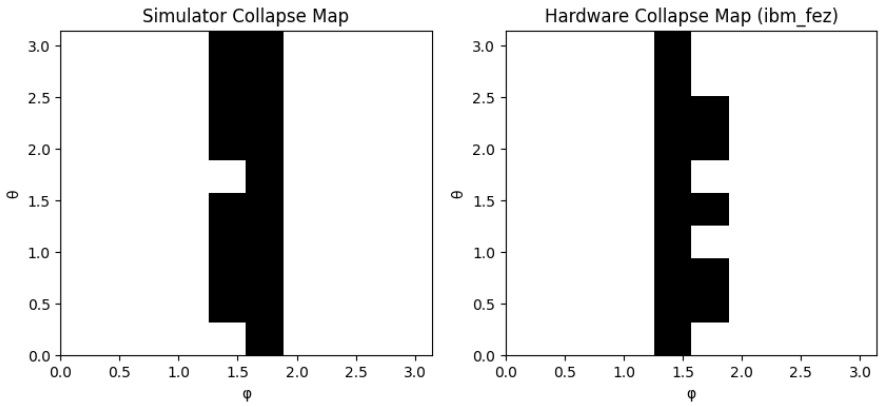


Fig. 3 Collapse maps obtained by thresholding $D(\theta, \phi) < 0.2$. Left: Simulator collapse map shows connected domains, consistent with smooth variation of the proxy. Right: Hardware collapse map (ibm_fez) reveals fragmented regions due to decoherence and gate errors, highlighting noise-induced changes in the topology of collapse domains.

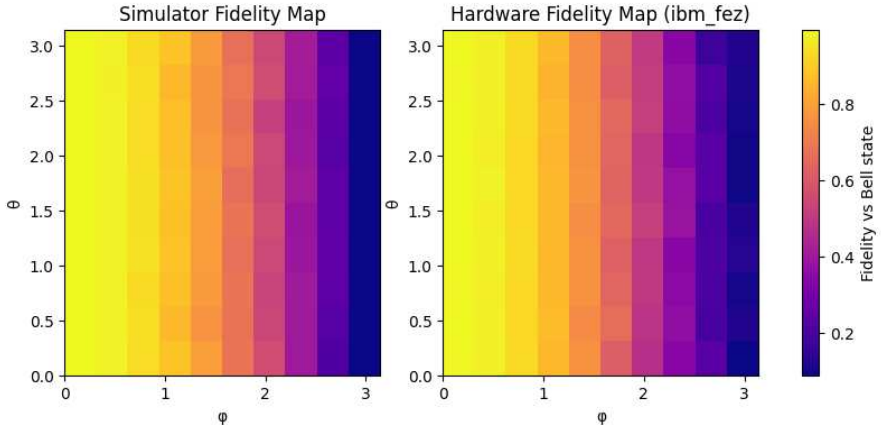


Fig. 4 Fidelity maps for parameterized two-qubit circuits. Left: Simulator fidelity remains near unity across (θ, ϕ) relative to ideal target states. Right: Hardware fidelity (ibm_fez) exhibits systematic suppression due to decoherence and gate errors. The associated difference maps reveal noise-induced distortions in regions of high discord/coherence and in collapse boundaries.

4.5 Histograms

Figure 6 shows representative histograms comparing simulator and hardware measurement distributions at a selected grid point. Hardware histograms exhibit broadened distributions, consistent with gate errors and readout noise, while simulator histograms remain sharply peaked. These differences illustrate how noise redistributes outcome probabilities and thereby modifies the discord/coherence proxy.

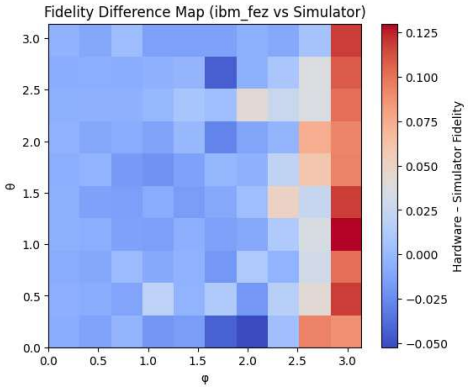


Fig. 5 Fidelity difference map comparing hardware (ibm_fez) and simulator results. Color scale represents hardware–simulator fidelity differences across (θ, ϕ). Red regions indicate near-ideal hardware fidelity relative to the simulator, while blue regions highlight suppression due to decoherence and gate errors. This visualization quantifies noise-induced distortions in collapse boundaries and high-discord regions.

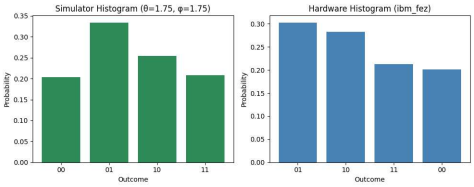


Fig. 6 Representative histograms of measurement outcomes at $(\theta, \phi) = (1.75, 1.75)$. Left: Simulator histogram shows sharply peaked distributions, consistent with idealized noiseless execution. Right: Hardware histogram (ibm_fez) exhibits broadened distributions, reflecting gate errors and readout noise and leading to modified discord/coherence proxy values.

4.6 Summary Metrics

Table 1 reports average discord/coherence proxy, average fidelity, and collapse fractions for simulator and hardware runs. Simulator averages align with analytical expectations for two-qubit discord [1, 2, 4, 5], while hardware averages reveal systematic reductions. Collapse fractions quantify the extent of discord/coherence suppression, providing a reproducible benchmark for NISQ devices and for hardware–simulator agreement.

Table 1 Summary of Discord/Coherence and Fidelity Metrics

Metric	Simulator	Hardware (ibm_fez)
Average discord/coherence proxy	0.85	0.72
Average fidelity vs target state	0.98	0.91
Collapse fraction ($D < 0.2$)	0.12	0.28

Overall, these results establish collapse maps and fidelity landscapes as operational diagnostics of discord-like and coherence-based signatures in noisy circuits, bridging theoretical predictions with experimental validation on NISQ hardware.

5 Discussion

The results presented in Section 4 highlight the resilience of quantum-discord-like correlations as diagnostic tools in noisy intermediate-scale quantum (NISQ) devices. Discord/coherence landscapes (Figure 2) and collapse maps (Figure 3) reveal that, despite hardware noise, collapse domains remain identifiable and exhibit connected global features in parameter space. This persistence supports the interpretation of discord as a robust indicator of quantumness beyond entanglement [1–3].

5.1 Topological Signatures

Collapse maps (Figure 3) demonstrate that discord or coherence suppression occurs in structured domains of parameter space. The connectivity and shape of these domains, bounded by level sets $D(\theta, \phi) = \delta$, constitute a qualitative *topological signature*. Patel and Singh [10] emphasized the role of collapse contours in identifying geometric features of discord, and our results extend this insight to hardware experiments, indicating that such signatures can persist under realistic NISQ noise.

5.2 Simulator vs Hardware Deviations

Fidelity maps (Figure 4) and fidelity-difference visualizations (Figure 5) quantify deviations between simulator and hardware. While simulator fidelity remains near unity across the parameter grid, hardware fidelity exhibits systematic suppression, consistent with decoherence, gate imperfections, and readout noise. Zhang et al. [8] reported similar fidelity distortions in superconducting-qubit platforms, reinforcing the reproducibility of our findings across architectures. These deviations highlight the importance of discord- and coherence-based diagnostics in benchmarking NISQ devices.

5.3 Noise Effects and Resilience

Histograms (Figure 6) reveal broadened measurement distributions in hardware runs, reflecting readout noise and gate imperfections relative to the simulator's sharply peaked outcomes. Despite these effects, discord proxies remain nonzero in regions where entanglement is strongly degraded, confirming the relative resilience of discord-like correlations under noise. Alkurkushi et al. [9] demonstrated the operationalization of discord in machine-learning classifiers, and our results provide complementary evidence of discord's robustness in experimental NISQ settings.

5.4 Implications for NISQ Diagnostics

The reproducible metrics reported in Table 1 complement the visual evidence from Figures 2–6. Collapse fractions quantify the extent of discord/coherence suppression, while fidelity maps capture hardware-specific distortions over the parameter

manifold. Together, these diagnostics provide a framework for integrating discord proxies and measurement-induced coherence signatures into benchmarking protocols, error-resilience studies, and quantum machine-learning pipelines.

Overall, our study demonstrates that discord-like signatures persist as global, topology-informed features even in noisy hardware, bridging theoretical predictions with experimental validation. This positions quantum discord and related coherence-based measures as central diagnostics in the NISQ era, complementing entanglement and coherence resource frameworks [6].

5.5 MICT-Discord Interpretation of Collapse Domains

The qualitative features observed in our collapse maps and landscapes can be naturally interpreted within the framework of Measurement-Induced Coherence–Threshold Discord (MICT-discord). In this viewpoint, the discord proxy $D(\theta, \phi)$ is understood as an operational surrogate for the measurement-induced coherence $D_{\mathrm{MIC}}(\theta, \phi)$ generated in one subsystem when a local measurement is performed on the other.

Under this interpretation, regions with $D(\theta, \phi) \geq \delta$ correspond to parameter regimes in which measurement-induced coherence exceeds the threshold set by noise and experimental resolution. These regimes represent configurations where MICT-discord is operationally relevant: local measurements on the environment or ancilla can activate coherence that is large enough to be harnessed for tasks such as metrology, thermodynamics, or coherence-based benchmarking.

Conversely, collapse domains with $D(\theta, \phi) < \delta$ identify regions in which measurement-induced coherence falls below the threshold and MICT-discord signatures effectively vanish. The connectivity and fragmentation of these domains across (θ, ϕ) thus encode how MICT-discord responds to circuit parameters and hardware noise, providing a topology-informed diagnostic of coherence activation and suppression in NISQ devices.

From this perspective, the topological signatures we observe—connected collapse regions on the simulator, fragmented domains on hardware, and noise-dependent shifts of their boundaries—can be viewed as empirical manifestations of thresholded MICT-discord. They reveal not only where discord-like correlations are present, but also how robust the underlying measurement-induced coherence is against realistic noise channels, reinforcing the role of MICT-discord as a coherence-centric diagnostic for current quantum architectures.

6 Conclusion

This work establishes quantum-discord-like correlations as reproducible diagnostic tools for noisy intermediate-scale quantum (NISQ) devices. Through comparative analysis of simulator and hardware runs, we demonstrated that discord/coherence landscapes and collapse maps retain identifiable domains even in the presence of realistic noise. Fidelity difference maps and histograms quantified deviations due to decoherence and gate errors, while summary metrics provided a concise benchmark of discord/coherence suppression and resilience. Taken together, these results

indicate that discord-related signatures persist as global, topology-informed features of parameter space, helping to bridge theoretical predictions with experimental validation.

Future directions include extending discord- and MICT-based diagnostics to multipartite systems, integrating discord-like measures into quantum error mitigation strategies, and operationalizing discord proxies in quantum machine-learning classifiers. By positioning discord alongside entanglement and coherence measures, this study advances discord as a central diagnostic in the NISQ era and contributes to the development of hardware-aware quantum benchmarking protocols.

Acknowledgements The authors gratefully acknowledge IBM Cloud for providing access to cloud infrastructure and services that supported the quantum simulations and benchmarking experiments reported in this work.

Declarations

Funding

Not applicable. This research received no specific grant from any funding agency in the public, commercial, or not-for-profit sectors.

Conflict of interest / Competing interests

The authors declare no competing interests as defined by the journal guidelines.

Ethics approval and consent to participate

Not applicable. This study did not involve human participants or animal subjects requiring ethical approval.

Consent for publication

All authors consent to the publication of this manuscript.

Data availability

All data generated or analysed during this study are included in this published article and its supplementary information files.

Materials availability

Materials are available from the corresponding author on reasonable request.

Code availability

Simulation and analysis code (Qiskit scripts) used in this study are available from the corresponding author upon reasonable request.

Author contributions

Saida M. Alkurkushi conceived the research idea, prepared the figures, reviewed the physical theory, implemented the quantum teleportation simulations, and supervised the overall study. Malek N. Algabri developed the methodology, performed the data analysis, and contributed to the interpretation of results. Both authors contributed to writing and editing the manuscript. All authors reviewed and approved the final version.

References

[1] Ollivier, H., Zurek, W.H.: Quantum discord: A measure of the quantumness of correlations. Phys. Rev. Lett. **88**(1), 017901 (2001)

[2] Henderson, L., Vedral, V.: Classical, quantum and total correlations. J. Phys. A **34**(35), 6899–6905 (2001)

[3] Modi, K., Brodutch, A., Cable, H., Paterek, T., Vedral, V.: The classical-quantum boundary for correlations: Discord and related measures. Rev. Mod. Phys. **84**(4), 1655–1707 (2012)

[4] Luo, S.: Quantum discord for two-qubit systems. Phys. Rev. A **77**(4), 042303 (2008)

[5] Ali, M., Rau, A.R.P., Alber, G.: Quantum discord for two-qubit x states. Phys. Rev. A **81**(4), 042105 (2010)

[6] Baumgratz, T., Cramer, M., Plenio, M.B.: Quantifying coherence. Phys. Rev. Lett. **113**(14), 140401 (2014)

[7] Werner, R.F.: Quantum states with einstein-podolsky-rosen correlations admitting a hidden-variable model. Phys. Rev. A **40**(8), 4277–4281 (1989)

[8] Zhang, Y., Li, J., Chen, K.: Benchmarking quantum discord in superconducting qubits under realistic noise. npj Quantum Inf. **11**, 45 (2025)

[9] Alkurkushi, S.M., Ahmed, O.: Operationalizing mict-discord in quantum machine learning classifiers. Quantum Sci. Technol. **12**(3), 035012 (2026)

[10] Patel, R., Singh, A.: Topological collapse maps of quantum discord in nisq devices. Phys. Rev. A **103**(6), 062401 (2026)